Motion Control of an Omnidirectional Mobile Robot with Steerable Omnidirectional Wheels

Kyung-Seok Byun*, Jae-Bok Song**

Dept. of Mechanical Eng., Korea Univ., Anam-dong, Sungbuk-gu, Seoul, 136-701, Korea
(Tel : 82-2-3290-3363; Fax : 82-2-3290-3357 ; E-mail: * byeonks@korea.ac.kr, **jbsong@korea.ac.kr)

Abstract: Omnidirectional mobile robots are capable of arbitrary motion in an arbitrary direction without changing the direction of wheels, because they can perform 3 degree-of-freedom (DOF) motion on a 2-dimensional plane. In this research, a new class of an omnidirectional mobile robot is proposed. Since it has synchronously steerable omnidirectional wheels, it is called an omnidirectional mobile robot with steerable omnidirectional wheels (OMR-SOW). It has 3 DOFs in motion and one DOF in steering. One steering DOF can function as a continuously variable transmission (CVT). CVT of the OMR-SOW increases the range of velocity ratio from the wheel velocities to robot velocity, which may improve performance of the mobile robot. The OMR-SOW with four omnidirectional wheels, have been developed in this research. Kinematics and dynamics of this robot is analyzed and motion control schemes of the robot are discussed in detail. Various tests have been conducted to demonstrate the validity and feasibility of the proposed mechanism and control algorithm. Experimental results show the OMR-SOW is successfully able to perform 2 translational motions, 1 rotational motion and 1 steering motion.

Keywords: Omnidirectional mobile robot, Motion control, Continuously variable transmission (CVT)

1. Introduction

Omnidirectional mobile robots are capable of moving in an arbitrary direction without changing the direction of wheels, because they can achieve 3 DOF motion on a 2-dimensional plane. Various types of omnidirectional mobile robots have been proposed so far; universal wheels [1, 2], ball wheels [3], off-centered wheels [4] are popular among them.

The omnidirectional mobile robots using omnidirectional wheels usually have 3 or 4 wheels.[5] It is desirable that four-wheeled vehicles be used when stability is of great concern.[6] However, independent drive of four wheels creates one extra DOF. To cope with such a redundancy problem, the mechanism capable of driving four omnidirectional wheels using three actuators was suggested. [7] Another approach to a redundant DOF is to devise some mechanism, which uses this redundancy to change wheel arrangements.[8, 9] It is called variable footprint mechanism (VFM). Since the relationship between the robot velocity and the wheel velocities depends on wheel arrangement, varying wheel arrangement can function as a continuously variable transmission (CVT) by adjustment of wheel arrangement without employing a gear train.

Most mobile robots have electric motors as actuators and battery as power source. Therefore, energy efficiency is of great importance in mobile robots because it is directly related to the operating time without charge. The transmission based on wheel arrangement, therefore, provides possibility of energy efficient drive. The CVT can provide more efficient motor driving capability as the range of its velocity ratio gets wider. The VFM proposed by Wada and Asada [8], however, has a limited range to ensure stability of a robot.

In a previous research, an omnidirectional mobile robot with steerable omnidirectional wheels (OMR-SOW) was proposed to improve CVT performance.[10] The OMR-SOW is an omnidirectional mobile robot with 3 DOF motion and 1 DOF in steering. The steering DOF can be achieved by synchronously steerable omnidirectional wheels. While the VFM has a common steering axis for all four wheels, the OMR-SOW has an independent steering axis for each wheel. Therefore, the OMR-SOW possesses a wider range of velocity ratio without stability degradation.

In this paper, motion control schemes for the motion of the OMR-SOW are discussed. OMR-SOW has 4 DOFs which are 2 translational motions, 1 rotational motion and 1 steering motion. These motions of the robot are controlled by velocity control or torque control of 4 wheels which are driven by motors. In this paper, two control methods are explained and compared. One is independent wheel velocity control and the other is computed torque control.

The remainder of this paper is organized as follows. In Section 2, kinematics and dynamics of the OMR-SOW are introduced. Section 3 explains motion control of the robot, and Section 4 shows experimental results and Section 5 concludes the research results.

2. Omnidirectional Mobile Robot with Steerable Omnidirectional Wheels

2.1 OMR-SOW

In this part, the structure and operational principle and control system of the proposed robot will be presented. Coordinate system of OMR-SOW is illustrated in Fig. 1. Notice that the four wheel modules can rotate about each pivot point C_1, .., C_4 located at the corners of the robot body, but they are constrained to have a synchronized steering motion of 1 DOF by the synchronous mechanism comprising the connecting links and linear guide.

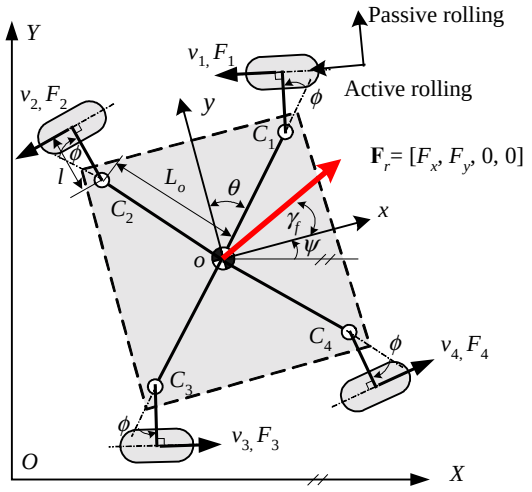

Fig. 1 Coordinate systems for omnidirectional mobile robot under consideration

In Fig. 1, the steering angle ϕ is defined as the angle from the zero position in which the lines (i.e., C_1C_3 or C_2C_4) connecting the centers of diagonally opposed wheels coincide with the diagonal lines of the robot body. Figure 2 shows various wheel arrangements.

(a) $\phi = -30^o$ (b) $\phi = 0^o$ (c) $\phi = +30^o$

Fig. 2 Various wheel arrangements of OMR-SOW.

The OMR-SOW was designed and constructed as shown in Fig. 3. This robot contains the wheel module comprising the four omnidirectional wheels connected to the individual motors, variable wheel arrangement mechanism, a square platform whose side is 500mm. The height of the platform from the ground is 330mm, and the motor drives and controller are placed on the platform.

The omnidirectional wheels used in the constructed mobile robot are called the *continuous alternate wheel* developed in our laboratory, where inner and outer rollers are arranged continuously, thus resulting in no gap between the rollers [11]. These wheels are connected to the DC motors through timing belts. A wheel suspension system is required to ensure that the wheels are in contact with the ground at all times. This suspension can also absorb the shock transmitted to the wheels.

Fig. 4 illustrates the control systems for the mobile robot. DSP (TMS320C31) is used as a master controller, while the microcontroller 80196KC is employed as a motor controller. The mobile robot can move autonomously, but the PC is used to monitor the whole system and collect data. The master controller plans the robot trajectory and commands the appropriate signal depending on the type of operation (i.e., speed mode or torque mode) to the motor drives where motor control is performed.

Fig. 3 Photo of OMR-SOW

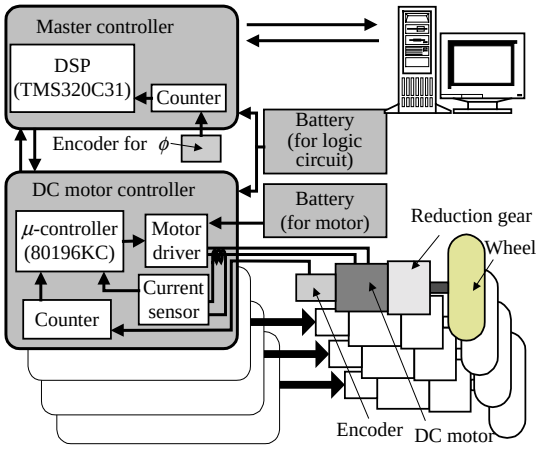

Fig. 4 Control systems for OMR-SOW

2.2 Kinematic analysis

As shown in Fig. 1, the frame *O-XY* is assigned as a reference frame for the robot motion in the plane and the moving frame *o-xy* is attached to the robot center. On the other hand, the angle θ between the *y*-axis and the diagonal line of the robot platform depends on the shape of a platform. (i.e., $\theta = 45^o$ for the square platform)

The relationship between the wheel velocity vector and the vehicle velocity vector can be expressed from the geometry in Fig. 1 by

$$\mathbf{V}_w = \mathbf{J}^{-1}\mathbf{V}_r, \quad \mathbf{V}_r = \mathbf{J}\,\mathbf{V}_w \tag{1}$$

where $\mathbf{V}_w = [v_1 \;\; v_2 \;\; v_3 \;\; v_4]^T$, $\mathbf{V}_r = [v_x \;\; v_y \;\; \dot{\psi} \;\; \dot{\phi}]^T$,

$$\mathbf{J} = \frac{1}{4}\begin{bmatrix} -1/C & -1/C & 1/C & 1/C \\ 1/S & -1/S & -1/S & 1/S \\ 1/L & 1/L & 1/L & 1/L \\ 1/l & -1/l & 1/l & -1/l \end{bmatrix}, \text{ where } \begin{cases} C = \cos(\theta - \phi) \\ S = \sin(\theta - \phi) \\ L = L_o \cos\phi + l \end{cases}$$

Here, v_1, v_2, v_3, v_4 are the wheel velocities in the active direction, v_x and v_y are the translational velocities of the robot center, $\dot{\psi}$ is the angular velocity about the robot center, and $\dot{\phi}$ is the derivative of the steering angle, respectively. **J** is the Jacobian matrix relating the wheel velocity vector to the robot velocity vector. The Jacobian is invertible, provided $0 < \theta - \phi < 90^o$ since $C \neq 0$ and $S \neq 0$. It follows from Eq. (1)

that the robot velocity and the steering velocity of the variable wheel arrangement mechanism can be completely determined by control of four independent motors driving each wheel.

2.3 Dynamic analysis

The dynamic model of the robot should be obtained for use in the CVT control algorithm. Consider the dynamic model of a robot shown in Fig. 1. The robot motion on the fixed coordinate system XY is described by

$$\mathbf{M}_r \dot{\mathbf{V}}_R = \mathbf{F}_R \tag{2}$$

where

$$\mathbf{M}_r = \begin{bmatrix} M & 0 & 0 & 0 \\ 0 & M & 0 & 0 \\ 0 & 0 & I_z & 0 \\ 0 & 0 & 0 & I_\phi \end{bmatrix}, \mathbf{V}_R = \begin{bmatrix} v_X \\ v_Y \\ \dot{\psi} \\ \dot{\phi} \end{bmatrix}, \text{ and } \mathbf{F}_R = \begin{bmatrix} F_X \\ F_Y \\ T_Z \\ T_\phi \end{bmatrix}.$$

where M is the mass of a robot, I_z the moment of inertia about the z-axis passing through the robot center and I_ϕ the moment of inertia about the steering axis of the wheel modules. Note that the subscript R represents the fixed reference coordinate system.

The transformation matrix from the moving to the absolute coordinate system is given by

$$\mathbf{R} = \begin{bmatrix} \cos\psi & -\sin\psi & 0 & 0 \\ \sin\psi & \cos\psi & 0 & 0 \\ 0 & 0 & 1 & 0 \\ 0 & 0 & 0 & 1 \end{bmatrix} \tag{3}$$

The relationship between the fixed reference frame and the moving robot frame is described by

$$\mathbf{V}_R = \mathbf{R} \cdot \mathbf{V}_r, \quad \mathbf{F}_R = \mathbf{R} \cdot \mathbf{F}_r \tag{4}$$

Differentiation of $\mathbf{V}_R$ is given by

$$\dot{\mathbf{V}}_R = \mathbf{R}\,\dot{\mathbf{V}}_r + \dot{\mathbf{R}}\,\mathbf{V}_r \tag{5}$$

Therefore, the robot of Eq. (2) is described on the moving coordinate system by

$$\mathbf{M}_r(\mathbf{R}\dot{\mathbf{V}}_r + \dot{\mathbf{R}}\mathbf{V}_r) = \mathbf{R}\mathbf{F}_r \quad \text{or} \quad \mathbf{R}^{-1}\mathbf{M}_r(\mathbf{R}\dot{\mathbf{V}}_r + \dot{\mathbf{R}}\mathbf{V}_r) = \mathbf{F}_r \tag{6}$$

On the other hand, the force and moment of a robot can be expressed from the geometry in Fig. 1 by

$$\mathbf{F}_r = \mathbf{J}^{-T}\mathbf{F}_w \quad \text{or} \quad \mathbf{F}_w = \mathbf{J}^T\mathbf{F}_r \tag{7}$$

where $\mathbf{F}_w = [F_1 \;\; F_2 \;\; F_3 \;\; F_4]^T$, $\mathbf{F}_r = [F_x \;\; F_y \;\; T_z \;\; T_\phi]^T$.

Here, $\mathbf{F}_x$ and $\mathbf{F}_y$ are the forces acting on the robot center in the x and y directions, T_z is the moment about the z axis passing through the robot center, and T_ϕ is the torque required to rotate the wheel modules, respectively. Note that the force F_i (i = 1,.., 4) is the traction force acting on the wheel in the direction of active rolling. It is noted that $\mathbf{F}_r$ is given by a vectorial sum of traction forces. Varying a combination of the traction forces can generate arbitrary forces and moments driving the vehicle and the moment steering the wheel modules.

In addition, the wheel forces are given by

$$R\mathbf{F}_w = \mathbf{U} - I_w\dot{\boldsymbol{\omega}}_w - c_w\boldsymbol{\omega}_w \text{ or } \quad R\mathbf{F}_w = \mathbf{U} - \frac{I_w}{R}\dot{\mathbf{V}}_w - \frac{c_w}{R}\mathbf{V}_w \tag{8}$$

where R is the wheel radius, $\mathbf{U} = [u_1 \;\; u_2 \;\; u_3 \;\; u_4]^T$ where u_i is the motor torque of the i-th motor, I_w is the moment of inertia of the wheel about the drive axis and c_w is the viscous friction factor of the wheel, and $\boldsymbol{\omega}_w = [\omega_1 \;\; \omega_2 \;\; \omega_3 \;\; \omega_4]^T$ where ω_i is the angular velocity of the i-th wheel. From Eq. (1), the wheel velocity and acceleration vectors are obtained by

$$\mathbf{V}_w = \mathbf{J}^{-1}\mathbf{V}_r, \quad \dot{\mathbf{V}}_w = \dot{\mathbf{J}}^{-1}\mathbf{V}_r + \mathbf{J}^{-1}\dot{\mathbf{V}}_r \tag{9}$$

After substitution of Eq. (7), (8) and (9) into (6), the following relation is obtained:

$$\mathbf{R}^{-1}\mathbf{M}_r(\mathbf{R}\dot{\mathbf{V}}_r + \dot{\mathbf{R}}\mathbf{V}_r) = \mathbf{J}^{-T}\mathbf{F}_w = \mathbf{J}^{-T}\frac{1}{R}\left(\mathbf{U} - \frac{I_w}{R}\dot{\mathbf{V}}_w - \frac{c_w}{R}\mathbf{V}_w\right)$$
$$= \mathbf{J}^{-T}\left(\frac{1}{R}\mathbf{U} - \frac{I_w}{R^2}(\dot{\mathbf{J}}^{-1}\mathbf{V}_r + \mathbf{J}^{-1}\dot{\mathbf{V}}_r) - \frac{c_w}{R^2}\mathbf{J}^{-1}\mathbf{V}_r\right) \tag{10}$$

This can be simplified by use of the relation $\mathbf{R}^{-1}\mathbf{M}_r\mathbf{R} = \mathbf{M}_r$ to

$$\mathbf{U} = (R\mathbf{J}^T\mathbf{M}_r + \frac{I_w}{R}\mathbf{J}^{-1})\dot{\mathbf{V}}_r$$
$$+ (R\mathbf{J}^T\mathbf{R}^{-1}\mathbf{M}_r\dot{\mathbf{R}} + \frac{I_w}{R}\dot{\mathbf{J}}^{-1} + \frac{c_w}{R}\mathbf{J}^{-1})\mathbf{V}_r \tag{11}$$

Eq. (11) represents the dynamic model of a robot. The above dynamic model neglected friction forces. The friction force term can be added to Eq. (6) to give

$$\mathbf{M}_r\dot{\mathbf{V}}_r + \mathbf{R}^{-1}\mathbf{M}_r\dot{\mathbf{R}}\mathbf{V}_r + \mathbf{f}_r = \mathbf{F}_r \tag{12}$$

where $\mathbf{f}_r$ represents the friction force and torque. Then, the dynamic model of Eq. (11) is modified to

$$\mathbf{U} = (R\mathbf{J}^T\mathbf{M}_r + \frac{I_w}{R}\mathbf{J}^{-1})\dot{\mathbf{V}}_r$$
$$+ (R\mathbf{J}^T\mathbf{R}^{-1}\mathbf{M}_r\dot{\mathbf{R}} + \frac{I_w}{R}\dot{\mathbf{J}}^{-1} + \frac{c_w}{R}\mathbf{J}^{-1})\mathbf{V}_r + R\mathbf{J}^T\mathbf{f}_r \tag{13}$$

2.4 Velocity and force ratios

Since the omnidirectional mobile robot is of 3 DOFs in the 2-D plane, it is difficult to define the velocity ratio in terms of scalar velocities. Thus the velocity ratio is defined using the concept of norms as follows:

$$r_v = \frac{\|\mathbf{V}_r\|}{\|\mathbf{V}_w\|} = \frac{\|\mathbf{J}\mathbf{V}_w\|}{\|\mathbf{V}_w\|} \tag{14}$$

The force ratio of the force acting on the robot center to the wheel traction force can be defined in the same way as the velocity ratio in Eq. (14) as follows:

$$r_f = \frac{\|\mathbf{F}_r\|}{\|\mathbf{F}_w\|} = \frac{\|\mathbf{J}^{-T}\mathbf{F}_w\|}{\|\mathbf{F}_w\|} \tag{15}$$

Note that the force ratio corresponds to the inverse of the velocity ratio. Fig. 5 shows the force ratio profiles as a

function of steering angle in the case of L_o = 0.283m, l = 0.19m, and θ = 45°. It is observed that the force ratio becomes maximum in one direction while minimum in the other direction as the steering angle reaches its maximum magnitude $\phi_{\max}$. Therefore, the steering angle should be determined so that the robot force to meet given specifications is generated. The translational force ratios vary significantly in the range between 0 and 2, while the rotational force ratio is kept nearly constant, when the steering angle is within the range between $-\phi_{\max}$ and $+\phi_{\max}$ ($0^o < \phi_{\max} < 45^o$). It is observed that the range of force ratio becomes wide as the steering angle grows in either sense.

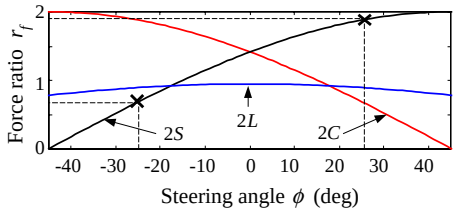

Fig. 5 Force ratio as a function of steering angle.

3. Motion Control

In this thesis, a robot is controlled by the independent wheel velocity control scheme requiring no model for the robot and the computed torque control method using the dynamic model developed in Section 2.

3.1 Independent wheel velocity control

The motion of a mobile robot can be controlled by wheel velocities. When the desired robot motion is given, the reference velocity of each wheel can be computed by Eq. (1) as follows

$$\mathbf{V}_{rref} = \mathbf{J}\,\mathbf{V}_{wref} \tag{16}$$

If each wheel is controlled to follow the reference velocity, then the robot can achieve the desired motion. Suppose that there is no slip between the wheel and the ground. The wheel velocity is represented by the angular velocity of a wheel and the radius of an omnidirectional wheel

$$\mathbf{V}_w = [v_1 \quad v_2 \quad v_3 \quad v_4]^T = R \cdot [\omega_1 \quad \omega_2 \quad \omega_3 \quad \omega_4]^T \tag{17}$$

Control of wheel velocity (thus the angular velocity of a wheel) can be performed by motor control. In this thesis, the wheel velocity is controlled to follow the reference velocity profile by a PI controller. Fig. 6 is shows the control system.

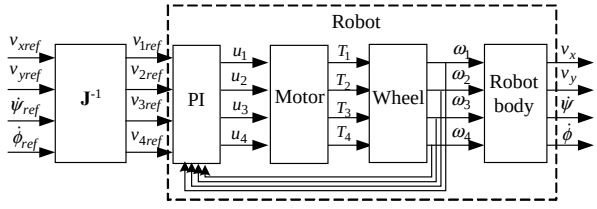

Fig.6 Independent wheel velocity control system

The system of Fig. 6 is based on the assumption of no slip. Practically, all mobile robots have slip between the wheels and the ground to some extent. This slip causes the real motion to be different from the desired one. The wheel velocity can be obtained by the wheel angular velocity in no slip condition, but this is not the case when slip exists. However, the velocity transmitted to the robot body by the wheel will still be called the wheel velocity even when slip arises. Suppose that the wheel velocity vector with slip is given by

$$\hat{\mathbf{V}}_w = [\hat{v}_1 \quad \hat{v}_2 \quad \hat{v}_3 \quad \hat{v}_4]^T \tag{18}$$

Then, the difference between the wheel velocity with no slip and that with slip is represented by

$$\tilde{\mathbf{V}}_w = \mathbf{V}_w - \hat{\mathbf{V}}_w \tag{19}$$

The difference of the robot velocity by slip is given from Eq. (1) as follows

$$\tilde{\mathbf{V}}_r = \mathbf{V}_r - \hat{\mathbf{V}}_r = \mathbf{J}\,\tilde{\mathbf{V}}_w \tag{20}$$

If an additional sensor (e.g., a gyroscope, vision system, ultrasonic sensor) measures robot motion, this error can be compensated for. Control for steering of the OMR-SOW when slip arises is discussed below.

If a steering angle is changed, a Jacobian of the OMR-SOW is also changed. Since the Jacobian affects all motions of the robot, the steering angle has to be controlled accurately. In case that there is a slip, measurement of the steering angle is needed to accurately control the angle. To measure a steering angle, an optical encoder is installed at the steering axis. In Eq. (20), the difference in steering angle by the slip is obtained by

$$\tilde{\dot{\phi}} = \dot{\phi}_{ref} - \dot{\phi} = \frac{1}{4l}(-\tilde{v}_1 + \tilde{v}_2 - \tilde{v}_3 + \tilde{v}_4) \tag{21}$$

The integration of this value is the error of steering angle. The reference steering velocity $\dot{\phi}_{ref}$ can be obtained by the difference between the reference steering angle ϕ_{ref} and the steering angle ϕ measured by the encoder as follows

$$\dot{\phi}_{ref} = K_\phi(\phi_{ref} - \phi) \tag{22}$$

where K_ϕ is the control gain of steering. If the reference steering angle is larger than the measured steering angle, the reference steering velocity has plus sign. The steering angle can follow the reference steering angle by proper control. Fig. 7 shows the control system with compensation for a steering angle.

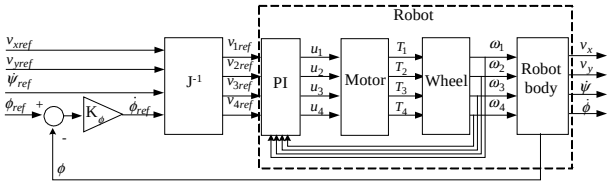

Fig. 7 Independent wheel velocity control system with compensation for steering angle

3.2 Computed torque control

The independent wheel velocity control scheme does not require the dynamic model. In this section, a control method based on a dynamic model is discussed.

Consider the robot dynamics in Eq. (13). If the desired robot

motion is given as $\mathbf{V}_{rd}$, the motor torque $\mathbf{U}$ which is the control input and causes $\mathbf{V}_r$ to follow $\mathbf{V}_{rd}$ should be computed. From Eq. (13), the control input can be obtained by feedback linearization as follows.

$$\mathbf{U} = (R\mathbf{J}^T\mathbf{M}_r + I_w\mathbf{J}^{-1})\dot{\mathbf{V}}_r^* + \left(R\mathbf{J}^T\mathbf{R}^{-1}\mathbf{M}_r\dot{\mathbf{R}} + \frac{I_w}{R}\dot{\mathbf{J}}^{-1} + \frac{c_w}{R}\mathbf{J}^{-1} \right)\mathbf{V}_r + R\mathbf{J}^T\mathbf{f}_r \quad (23)$$

where $\dot{\mathbf{V}}_d^*$ is given by

$$\dot{\mathbf{V}}_r^* = \dot{\mathbf{V}}_{rd} + 2\boldsymbol{\lambda}\,\mathbf{e}_v + \boldsymbol{\lambda}^2\int_0^t \mathbf{e}_v dt \quad (24)$$

the velocity error is defined by

$$\mathbf{e}_v = \mathbf{V}_{rd} - \mathbf{V}_r \quad (25)$$

and $\boldsymbol{\lambda}$ is the control gain as follows

$$\boldsymbol{\lambda} = \begin{bmatrix} \lambda_1 & 0 & 0 & 0 \\ 0 & \lambda_2 & 0 & 0 \\ 0 & 0 & \lambda_3 & 0 \\ 0 & 0 & 0 & \lambda_4 \end{bmatrix} \quad (26)$$

If the control input in Eq. (23) is substituted into the dynamic model of Eq. (13), the error dynamics is obtained as

$$\dot{\mathbf{V}}_r^* - \dot{\mathbf{V}}_r = \dot{\mathbf{e}}_v + 2\boldsymbol{\lambda}\,\mathbf{e}_v + \boldsymbol{\lambda}^2\int_0^t \mathbf{e}_v dt = 0 \quad (27)$$

Thus, if $\lambda_i > 0$, $\mathbf{V}_r$ follows $\mathbf{V}_{rd}$ in a stable manner. Fig. 8 shows this control system, where $\hat{\mathbf{D}}_{robot}^{-1}$ denotes the inverse dynamic model of the robot.

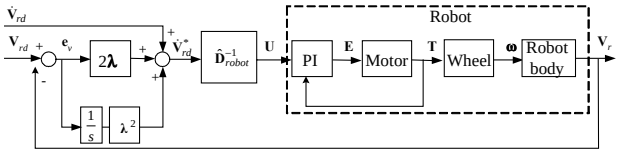

Fig. 8 Computed torque control system

For implementation of the control law in Eq. (23), a friction model is required. When the robot velocity is constant, Eq. (12) is simplified to

$$\mathbf{f}_r = \mathbf{F}_r - \mathbf{R}^{-1}\mathbf{M}_r\dot{\mathbf{R}}\mathbf{V}_r \quad (28)$$

From (7) and (8), $\mathbf{F}_r$ becomes

$$\mathbf{F}_r = \mathbf{J}^{-T}\mathbf{F}_w = \mathbf{J}^{-T}\left(\frac{1}{R}\mathbf{U} - \frac{c_w}{R^2}\mathbf{J}^{-1}\mathbf{V}_r \right) \quad (29)$$

Note that the robot velocity is assumed to be constant in Eq. (29). Thus the friction force is obtained by

$$\mathbf{f}_r = \frac{1}{R}\mathbf{J}^{-T}\mathbf{U} - \left(\frac{c_w}{R^2}\mathbf{J}^{-T}\mathbf{J}^{-1}\mathbf{V}_r + \mathbf{R}^{-1}\mathbf{M}_r\dot{\mathbf{R}} \right)\mathbf{V}_r \quad (30)$$

From experimental results for friction model and Eq. (30), the friction model is obtained by

$$\mathbf{f}_r = \left[f_x \operatorname{sgn}(v_x) \quad f_y \operatorname{sgn}(v_y) \quad \tau_\psi \operatorname{sgn}(\dot{\psi}) \quad \tau_\phi \operatorname{sgn}(\dot{\phi}) \right]^T \quad (31)$$

where f_x = (18.5 + 7.0ϕ) N, f_y = (18.5 - 7.0ϕ) N, τ_ψ = 6.20 Nm and τ_ϕ = 3.05 Nm.

If the control input compensates for the friction force using the model, control performance can be improved. Because of the sign function of friction model and backlash of the mechanism, however, the system may be unstable or may occur dithering. To solve this problem, saturation function is used in the friction model

4. Experiments and Discussions

As explained in Section 2, the OMR-SOW has 2 DOF translations, 1 DOF rotation and 1 DOF steering, all of which are obtained by control of 4 motors. The independent wheel velocity control and the computed torque control schemes have been applied to motion control of the OMR-SOW.

If the desired robot motion is given, each wheel velocity for this motion can be obtained from Eq. (1). Each motor is controlled for the wheel to follow the commanded velocity by a PI control scheme. Fig. 9 shows experimental results for a square trajectory using the independent wheel velocity control scheme. Fig. 9(a) shows robot velocity and steering angle. The robot velocity follows the reference input faithfully. Since the accumulated position error is not compensated for, however, there is a position error between the reference and actual trajectory. Fig. 9(b) shows each wheel velocity and motor currents.

The independent wheel velocity control cannot compensate for a steering angle error caused by disturbance and/or slip. Fig. 10 shows an experiment to emphasize this feature of the control system. While a robot moves in the x direction, it encounters an obstacle of 4cm in height and surmounts it. The slip introduced by this obstacle causes the steering angle to change as shown in Fig. 10. The robot is able to adjust steering so as to follow the reference input and thus robot velocity can maintain the desired values event after the obstacle. However, steering angle is not returned to the previous angle.

In the experiment of Fig. 11, the control system uses the independent wheel velocity control with feedback of a steering angle. The steering angle is measured and the error between the measured and the desired steering angle is corrected by the steering velocity which is proportional to the error. The steering angle is changed by an obstacle, but it returns to the previous angle. Therefore, using the control system with steering feedback, the robot can be driven with desired steering angle even if disturbance and/or slip occur.

Implementation of independent wheel velocity control needs only gain tuning of the controller for each wheel without information about the robot. Though the robot velocity can be controlled and the steering angle can be compensated for by feedback, however, the position error of a robot cannot be compensated for. On the other hand, the computed torque control scheme has an integral term of the velocity error (i.e., position error), as in Eq. (24). Thus, the position of the robot including steering angle can be controlled. Fig. 12 shows the results using the computed torque control scheme. The steering angle keeps its original angle without additional feedback.

5. Conclusions

In this research, an omnidirectional mobile robot with steerable omnidirectional wheels (OMR-SOW) has been proposed and the kinematic and dynamic analysis of a proposed robot has been conducted. The OMR-SOW has 4 DOFs which consist of 3 DOFs for omnidirectional motion and 1 DOF for steering. This steering DOF functions as a continuously variable transmission (CVT). Therefore, the OMR-SOW can be also considered as an omnidirectional mobile robot with CVT. The OMR-SOW was constructed and tested.

Two motion control schemes were developed and various experiments were conducted. One is the independent wheel velocity control with compensation for steering angle and the other is the computed torque control scheme which uses the dynamic model of a robot. By the motion control system, the OMR-SOW has successfully performed 4 DOF motions which are 2 translational motions, 1 rotational motion and 1 steering motion.

References

[1] J. F. Blumrich, "Omnidirectional vehicle," *United States Patent* 3,789,947, 1974.

[2] B. E. Ilou, "Wheels for a course stable self-propelling vehicle movable in any desired direction on the ground or some other base," *United States Patent* 3,876,255, 1975.

[3] M. West and H. Asada, "Design of ball wheel mechanisms for omnidirectional vehicles with full mobility and invariant kinematics," *Journal of mechanical design*, Vol. 119, pp.153-161, 1997.

[4] M. Wada and S. Mory, "Holonomic and omnidirectional vehicle with conventional tires," *Proc. of ICRA*, pp. 3671-3676, 1996.

[5] S. Saha, J. Angeles, and J. Darcovich, "The kinematic design of a 3-dof isotropic mobile robot," *Proc. of ICRA*, pp.283-288, 1993.

[6] P. Muir and C. Neuman, "Kinematic modeling of wheeled mobile robots," *Journal of Robotic Systems*, Vol. 4, No. 2, pp. 281-340, 1987.

[7] H. Asama, M. Sato, L. Bogoni, H. Kaetsu, A. Masumoto, and I. Endo, "Development of an omnidirectional mobile robot with 3 DOF decoupling drive mechanism," *Proc. of ICRA*, pp. 1925-1930, 1995.

[8] M. Wada and H. Asada, "Design and control of a variable footprint mechanism for holonomic omnidirectional vehicles and its application to wheelchairs," *IEEE Transactions on Robotics and Automation*, Vol. 15, No. 6, pp. 978-989, 1999.

[9] K. Tahboub and H. Asada, "Dynamic analysis and control of a holonomic vehicle with continuously variable transmission," *Proc. of ICRA*, pp. 2466-2472, 2000.

[10] K.S. Byun, S.J. Kim and J.B. Song, "Design of a Four-Wheeled Omnidirectional Mobile Robot with Variable Wheel Arrangement Mechanism," *Proc. of ICRA*, pp.720-725, 2002.

[11] K.S. Byun, S.J. Kim and J.B. Song, "Design of continuous alternate wheels for omnidirectional mobile robots," *Proc. of ICRA*, pp. 767-772, 2001.

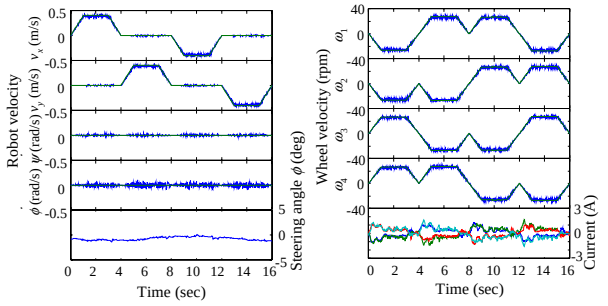

(a) $\mathbf{V}_r$ and ϕ (b) $\boldsymbol{\omega}$ and $\mathbf{U}$

Fig. 9 Experiment for square trajectory using independent wheel velocity control

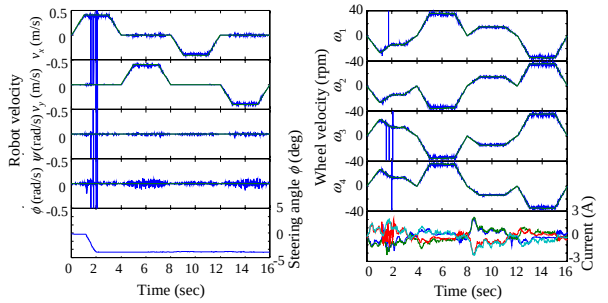

(a) $\mathbf{V}_r$ and ϕ (b) $\boldsymbol{\omega}$ and $\mathbf{U}$

Fig. 10 Experiment for square trajectory with obstacle using independent wheel velocity control

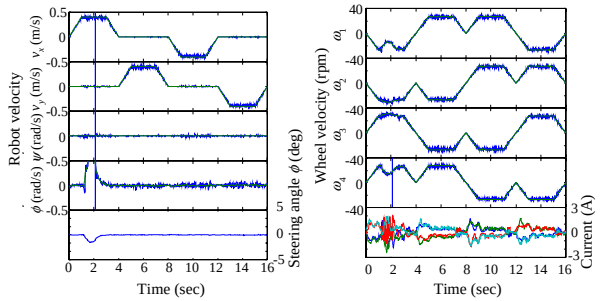

(a) $\mathbf{V}_r$ and ϕ (b) $\boldsymbol{\omega}$ and $\mathbf{U}$

Fig. 11 Experiment for square trajectory with obstacle using independent wheel velocity control with feedback of steering angle

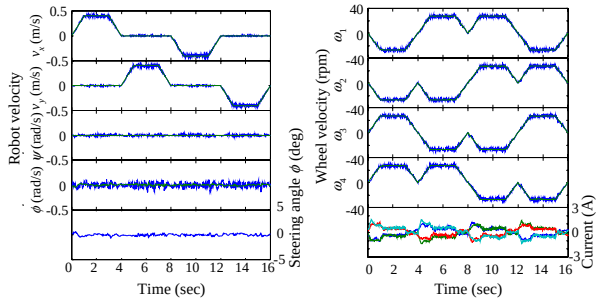

(a) $\mathbf{V}_r$ and ϕ (b) $\boldsymbol{\omega}$ and $\mathbf{U}$

Fig. 12 Experiment for square trajectory using computed torque control